



# Diffuse reflection inside a hexagonal nanocavity

Nengwen Wang\*<sup>†</sup>, Xiaodong Chen\*, Yuhua Yang\*, Jianwen Dong, Chengxin Wang & Guowei Yang

State Key Laboratory of Optoelectronic Materials and Technologies, Institute of Optoelectronic and Functional Composite Materials, Nanotechnology Research Center, School of Physics & Engineering, Sun Yat-sen University, Guangzhou 510275, Guangdong, P. R. China.

SUBJECT AREAS:

OPTICAL PHYSICS

NANOSCALE MATERIALS

MATERIALS FOR OPTICS

APPLIED OPTICS

Received  
12 November 2012

Accepted  
30 January 2013

Published  
18 February 2013

Correspondence and requests for materials should be addressed to G.W.Y. (stsygw@mail.sysu.edu.cn) or J.W.D. (dongjwen@mail.sysu.edu.cn)

\* These authors contributed equally to this work.

<sup>†</sup> Current address: Shanghai Institute of Optics and Fine Mechanics, Chinese Academy of Sciences, Shanghai 201800, P. R. China.

Geometrical diffuse reflection is a common optical phenomenon that occurs when a reflecting surface has roughness of order of hundreds of micrometres. Light rays thus reflect uniformly in all directions with each ray obeying Snell's law. Of interest is knowing what happens when light reflects off surfaces with roughness of nanometres. Here, by introducing nanoscaled roughness on the hexagonal faces of ZnO nanocavities, we observe luminescent profiles with flowery patterns, replacing the usual whispering gallery modes. The unique profile for these nanocavities is attributed to wave diffuse reflection, which occurs when the features on the reflecting surfaces are typically nanometre-sized. Light with wavelengths of similar scale “sees” these nano-perturbations, and undergoes scattering rather than geometrical diffuse reflection. These findings could benefit the fields of nanoscale topography and nanoscopic uniform lighting by using wave diffuse reflection.

Diffuse reflection is a well-known but important optical phenomenon that is commonly observed in daily life<sup>1</sup>. Light reflects and diffuses in many different directions from surfaces that are microscopically rough with features typically the size of hundreds of micrometres. In general, light reflects according to the geometrical law of reflection. As a result of the random orientation of the microscale surfaces, light rays have almost equivalent intensity in all reflected directions, causing geometric diffuse reflection to occur. However, we are interested in whether diffuse reflection appears when the typical sizes of features on a reflecting surface are of nanoscale orders. Unfortunately, this fundamental issue has no intuitive picture based in theory to explore light propagation on such surfaces. Also of interest is knowing whether reflected light still has a uniform intensity in all directions, and what new physics happens on nanoscale-rough surfaces. Additionally, random surface studies are of great interest to researchers in fields such as dynamical localisation in chaotic microdisks<sup>17,18</sup>, surface plasmons<sup>2</sup>, second-harmonic generation<sup>3</sup>, and Raman scattering<sup>4</sup>. Random surfaces are also widely investigated in research on topography<sup>5</sup> and topology<sup>6</sup>. In our study, we fabricated a series of hexagonal ZnO nanocavities with nanoscaled roughness and observed unique luminescent profiles with novel flowery patterns.

Generally, in a hexagonal ZnO nanocavity, light is confined because of multiple total internal reflections along the boundary of the optical resonator, and the distribution of luminescence intensity is locally concentrated at the hexagonal faces, which directly result in typical luminescence enhanced by whispering gallery modes (WGMs)<sup>7–9</sup>. However, by introducing nanoscaled roughness on these faces, we can see a new kind of diffuse reflection, namely wave diffuse reflection, occurring as light reflects from sample faces under conditions where total internal reflection no longer holds causing the WGMs to disappear. In place, other interesting modes emerge with highly symmetric flowery profiles. In this configuration, light “sees” the nanoscale roughness as both light and roughness are of the same length order, and Snell's law is no longer valid on such surfaces. Experiments, theoretical analysis, and computer modelling performed in our study have demonstrated that the WGMs are not generated in these nanoscale-rough nanocavities; instead, wave diffusion reflection occurs as electromagnetic (EM) waves reflect in all possible directions. The reflected light has an almost uniform intensity in all directions, and no obvious reflecting angle can be defined. A new kind of flowery luminescent pattern appears because of reflections occurring on the smooth surface in the six corners of the hexagonal ZnO nanocavity. Importantly, this kind of interesting luminescent pattern can be observed by using a rigorous finite element method, and can be understood in a simple geometrical manner.

## Results

The hexagonal ZnO nanocavities are prepared on silicon wafers using simple thermal chemical vapour transport and condensation without any metal catalysts<sup>10,11</sup>. Four typical hexagonal ZnO nanocavities of various size and

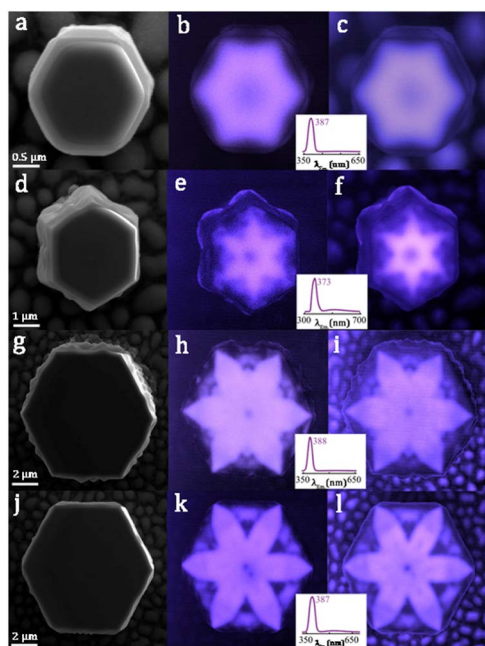


**Figure 1** | (a), (d), (g), (j), SEM images (top view) of four typical hexagonal ZnO nanocavities of different sizes and nanoscaled surface roughness. (b), (e), (h), (k), the corresponding panchromatic CL images, and (c), (f), (i), (l), the monochromatic CL images (around 386 nm), in which we clearly see different petaline luminescent patterns resulting from the differences in size and roughness. The insets between the two CL images are the corresponding CL spectra.

nanoscaled roughness (Fig. 1) were selected to pursue the diffuse reflection inside hexagonal nanocavities. Geometrically, all hexagonal nanocavities are columns, and have a near-perfect and smooth hexagonal top surface and six faces with different nanoscaled roughness. From the cathodeluminescence (CL) images from inside these ZnO nanocavities, the luminescent profiles clearly show novel hexagonal petaline patterns (Figs. 1b, e, h and k). The geometrical shape of these petals are slightly different because of differences in size and roughness of nanocavities. The roughness of the six faces has a great influence on the luminescent pattern (see for example Figs. 1h and k). We emphasise that the only difference between the ZnO nanocavities generating WGM patterns and our samples with petaline luminescent pattern is introducing nanoscaled roughness on the six faces (Figs. 1a, d, g and j). For typical WGM nanocavities, the faces are smooth (see Supplementary information). When light impinges on these faces, total internal reflection takes places and results in well-defined WGMs with high fidelity. However, when the faces have nanoscaled roughness, light feels out the nano-scale perturbations complicating reflection. The reflection intensity will vary considerably, and the reflected path will no longer be centred on the geometrical angle of reflection. Instead, our observations reveal that the behaviour of light in these circumstances undergoes wave diffuse reflection, in analogy to geometrical optical phenomenon, but governed by scattering theory rather than geometrical ray optics.

## Discussion

To understand wave diffuse reflection, consider a one-dimensional nanoscaled rough surface between ZnO and air in the context of the extinction theorem<sup>12–15</sup>. Two length scales are used to characterise the statistical properties of features in the rough surface. One is the root-mean-square (RMS) of surface heights  $\sigma$ ; the larger  $\sigma$  is, the higher the maximum height of the surface is. Another is the correlation length  $T$ ; the smaller  $T$  is, the more the surface fluctuates. We study the reflected behaviour (both reflectance and angular reflected

intensity) of light with incident angle  $\theta_0$  (for more information, see Supplementary Information). Here, we assume that the permittivity of ZnO is constant,  $\epsilon = 5.29^{16}$ , and the wavelength inside ZnO is  $\lambda = 186$  nm, corresponding to the CL peaks in Fig. 1.

Fig. 2a shows the variation of the reflectance at different incident angles for s-polarised light incident on a ZnO surface; p-polarised light behaves similarly. When the surface is smooth, i.e.,  $\sigma = 0$ , Snell's Law is satisfied. The reflectance slowly increases at small incident angles but notably increases near the critical angle  $\theta_c$  ( $\theta_c = \sin^{-1}(\sqrt{\frac{1}{\epsilon}}) \approx 25^\circ$ ); total internal reflection occurs at  $\theta_0 > \theta_c$ . Given a nanoscale-rough surface (a nano-perturbation), some interesting EM behaviour related to wave diffuse reflection is observed. If  $\sigma$  is sufficiently large, the reflectance no longer becomes unity at  $\theta_0 > \theta_c$ . For example, the reflectance decreases to 0.8 at  $\theta_0 = 30^\circ$  when  $\sigma$  reaches  $0.5\lambda$  (green in Fig. 2a). Furthermore, for small incident angles, the reflectance from a large rough surface (e.g.  $\sigma = \lambda$ ) will be several times greater than from a smooth surface of the same material, inferring that reflectance changes slowly for all incident angles from large rough surfaces. Typically, when the correlation length and the RMS deviation are set to  $4.4\lambda$  and  $4\lambda$ , respectively, reflectance is almost at 0.8 (pink in Fig. 2a). Note that reflectance just describes the total reflected power flow in all backward angles, but it does not indicate what the angular intensity distribution is of the reflected light. Although the reflectance is the same for different rough surfaces, the angular intensity distributions will exhibit distinctly different profiles, which is another key characteristic of wave diffuse reflection.

Figs. 2b and c show reflectance phase diagrams with respect to  $(T, \sigma)$ , so as to provide a full picture of wave diffuse reflection. We focus on incident angles  $30^\circ$  and  $60^\circ$  as these are related to the respective quasi-WGMs and WGMs of hexagonal ZnO nanocavities.

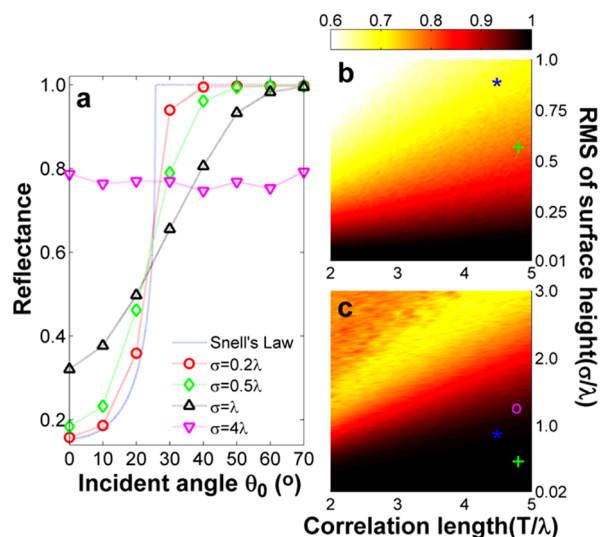


**Figure 2** | Reflectance in the combination of  $(T, \sigma)$ . (a), Reflectance from the nanoscale rough ZnO surfaces with different incident angles for different values of  $\sigma$ . The length  $T$  is fixed at  $4.4\lambda$  to simulate a representative example. The RMS deviations  $\sigma$  are set to  $0.2\lambda$  (red),  $0.5\lambda$  (green), and  $\lambda$  (black) to simulate different nanoscale roughness. The reflectance of the smooth surface (blue), which notably increases around the critical angle  $\theta_c$ , is drawn for comparison. b and c, phase diagrams for the incident angle  $\theta_0$  to be  $30^\circ$  and  $60^\circ$ , respectively, b which is related to quasi-WGM and WGM of hexagonal ZnO nanocavities. Similar colour changes are found in (b) and (c), except that low reflectance occurs at larger  $\sigma$  in c than in (b). The characteristics for the samples imaged in Figs. 1a, 1d, 1g are marked in (b) and (c) with coloured symbols of a green plus, blue asterisk, and purple circle, respectively.



Similar rules can be observed in both phase diagrams. The reflectance is high when the reflected surface is a little rough (small  $\sigma$  marked as black regions in Figs. 2b and c). As  $\sigma$  increases, the reflectance drops gradually (colour changes from black to white). For example, the reflectance is lower than 0.6 when  $\sigma$  exceeds  $0.5 \lambda$  in Fig. 2b, indicating a large transmission of energy across the surface into air. A similar behaviour can be seen in Fig. 2c except that the low reflectance occurs at larger  $\sigma$ . We recall that the two phase diagrams are related to both types of WGMs in the hexagonal ZnO nanocavity. Therefore, as the lengths of the surface features of our experimental samples are within the low-reflectance regime, it is reasonable to argue that both WGM resonance conditions no longer are valid when roughness is sufficiently large. This is why strong luminescence is not observed at the boundary of the rough ZnO nanocavities, illustrated in the first three rows of Fig. 1. Additionally, nano-rough surfaces with high reflectance (e.g.  $\sigma \sim 0.5 \lambda$  in Fig. 2c) do not guarantee the generation of WGMs in hexagonal nanocavities. This is because the reflected energy can have a homogeneous distribution in backward directions (this point will be discussed in the next paragraph). Overall, both the quasi-WGMs and WGMs cannot survive in hexagonal ZnO nanocavities with surfaces that are sufficiently rough.

As mentioned above, the angular intensity distribution is another key feature in wave diffuse reflection. Here, we focus on situations with  $T = 4.4 \lambda$ . The relationships between reflected intensity and reflected angle are presented for the quasi-WGM and WGM (Figs. 3a and b respectively). For low  $\sigma$ , the reflection intensity is centred

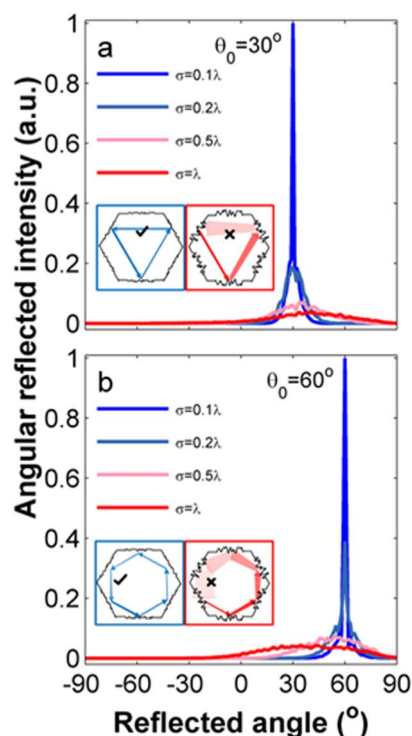


**Figure 3** | (a) and (b), Distribution of angular reflected intensity at the incident angle of  $30^\circ$  and  $60^\circ$ , respectively.  $\sigma$  is set to  $0.1 \lambda$  (dark blue),  $0.2 \lambda$  (light blue),  $0.5 \lambda$  (purple), and  $\lambda$  (red). When  $\sigma$  is small (dark blue), the reflected intensity concentrates at the geometrical reflection angle. When  $\sigma$  is large enough (purple or red curve), the reflected intensity has a homogeneous distribution over  $-90^\circ$ – $90^\circ$ . Blue (red) inset indicates the survival (colour fade) for a quasi-WGM and a WGM with small (large) nanoscale perturbations present. In the insets, the width of the light beam represents the angle of divergence; the width becomes larger if reflection becomes wave diffused. The intensity of colour represents the energy of light; the darker the colour, the more energy carried by the light beam.

narrowly about the geometrical reflection angle, signifying that Snell's law ensures both types of WGMs survive. In Fig. 3, the two blue-framed insets show that the width of light beam and the colour remains unchanged, inferring that most of the incident light undergoes specular reflection. The trajectory of light is still well defined, and thus no wave diffuse reflection exists. However, with sufficiently large  $\sigma$  (e.g.  $\sigma = 0.5 \lambda$  or  $\lambda$ ), the reflection intensity is almost uniformly distributed in all directions from  $-90^\circ$  to  $90^\circ$ , and the peak values are low enough to suppress the quality factor for both types of WGM. That is, incident light undergoes wave diffuse reflection rather than specular reflection. Conditions required for total internal reflection vanish, and the quasi-WGMs and WGMs no longer propagate in the hexagonal ZnO nanocavity with large roughness. The two red insets depict the light beam becoming increasingly wider, and because of energy leakage, its colour changes from dark red to light red.

Which modes ultimately survive and emerge once both WGMs disappear? Obviously, this is not a simple question to answer because there are many eigenmodes in the rough hexagonal ZnO nanocavity with lifetimes of the same order. For rigour, a full vectorial EM method should be developed to determine the field patterns within a rough hexagonal nanocavity. Here, we use the commercially available finite element software (COMSOL Multiphysics) to undertake a simulation. Given our computational resources, we set the sample size to  $2430 \text{ nm}$  and set the two length scales associated with surface roughness to  $T = 0.1 \lambda$  and  $\sigma = 0.2 \lambda$ . Interestingly, for a rough hexagonal nanocavity, one of the numerical eigenmode patterns (see the total electric field pattern in Fig. 4a) is consistent with experimental observations. Indeed, with different nanocavity sizes, many kinds of flowery modes are observed in the samples (Fig. 1). To understand these modes in a simple manner, we propose one possible light path for one kind of flowery luminescent pattern in a large sample (Fig. 4b). As the corners in a hexagonal ZnO nanocavity are flat and smooth, wave diffusion reflection does not occur and the law of total internal reflection still holds. There are thus two possible quasi-WGM light path branches, as indicated by blue and green dashed lines in Fig. 4b. These orbits avoid the rough faces and have a rotated counterpart, which together produce the flowery pattern. Note that this is not the same as the six-bounce orbit, which produces the hexagram pattern rather than a petaline pattern<sup>19</sup>. Indeed, after being reflected at every corner of the hexagonal nanocavity, light returns to the starting point forming a closed loop composed of alternating long diagonal and short lateral paths around the nanocavity. As a result, in addition to the flowery pattern, we should see a bright ring around boundary of the sample, as evident in the image of Fig. 1i.

In summary, by introducing nanoscaled roughness on the hexagonal faces of a ZnO nanocavity, we observe a new kind of diffuse

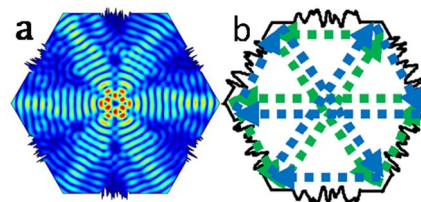


**Figure 4** | (a), Numerical simulation (domain of ZnO section) of total electric field of hybrid mode of one of rough ZnO samples at wavelength around  $386 \text{ nm}$ . (b), Schematic for one possible light path of the flowery luminescent pattern. There are two possible quasi-WGM light path branches (each has a rotated counterpart): one is indicated by green, the other by blue. After being reflected at every corner of the hexagonal ZnO sample, light returns to the initial starting point forming a complete, closed loop. Along with the bright ring around the sample boundary, the petaline luminescent pattern is then formed.





reflection, namely wave diffuse reflection. Nano-roughness breaks the conditions required for total internal reflection and suppresses the WGMs; in place, other modes emerge, generating flowery petal-like profiles with concomitant symmetry of the nano-cavity. These discoveries of wave diffuse reflection open up new prospects in nanoscale topography and nanoscopic uniform lighting.

## Methods

Following procedures detailed in our previous works<sup>10,11</sup>, a variety of ZnO nanostructures have been prepared on single-crystal silicon wafers. These nanostructures grow vertically from the substrate and are sparsely dispersed. In brief, a mixture of ZnO and graphite powders was loaded on one end of an alumina plate. Next, at the other end, single-crystal silicon wafers were placed. The alumina plate was then put inside a small quartz tube, and this system was placed in a horizontal quartz-tube electric furnace. The system was rapidly heated to 1050°C and held at this temperature for 20–40 min in an argon atmosphere, which was maintained by a flow rate of 50 SCCM under a pressure of  $2 \times 10^4$  Pa. Finally, the source powders and silicon wafers were removed from the furnace and rapidly cooled in air. A grey film was observed on the substrates. Note that we can control the shape and size of the as-prepared sample by preparation parameters such as pressure and temperature.

The CL measurements of the ZnO nanostructures were performed at room temperature using a Gatan Mono-CL system attached to a field emission scanning electron microscope (FESEM) with an accelerating voltage of 10 kV. The focus electron beam was used as excitation source to excite samples. A collector probe and a spectro-analysis instrument collected and processed the fluorescence signals. Note that with nano-size materials, spatially resolved CL microscopy is so far the only effective technique to characterise the optical properties of each individual nanostructure<sup>10,11</sup>.

We used the pre-set study of eigenfrequency in the RF module of COMSOL Multiphysics engineering simulation software to analyse the eigenmodes of hexagonal ZnO samples with nanoscale roughness. Two-dimensional geometry was used. The dielectric constant of the hexagonal ZnO samples is 5.29. Continuous boundary conditions were set at the interface between ZnO sample and air. We searched modes for which wavelengths were around 386 nm.

1. Born, M. & Wolf, E. *Principles of Optics: Electromagnetic Theory of Propagation, Interference and Diffraction of Light* 7th edn, Ch. 1 (Cambridge University Press, Cambridge, 1999).
2. Kretschmann, E., Ferrell, T. L. & Ashley, J. C. Splitting of the Dispersion Relation of Surface Plasmons on a Rough Surface. *Phys. Rev. Lett.* **42**, 1312–1314 (1979).
3. Chen, C. K., de Castro, A. R. B. & Shen, Y. R. Surface-Enhanced Second-Harmonic Generation. *Phys. Rev. Lett.* **46**, 145–148 (1981).
4. Garcia-Vidal, F. J. & Pendry, J. B. Collective Theory for Surface Enhanced Raman Scattering. *Phys. Rev. Lett.* **77**, 1163–1166 (1996).
5. Sayles, R. S. & Thomas, T. R. Surface topography as a nonstationary random process. *Nature* **271**, 431–434 (1978).
6. Banavar, J. R., Maritan, A. & Stella, A. Geometry, topology, and universality of random surfaces. *Science* **252**, 825–827 (1991).
7. Nobis, T., Kaidashev, E. M., Rahm, A., Lorenz, M. & Grundmann, M. Whispering gallery modes in nano-sized dielectric resonators with hexagonal cross section. *Phys. Rev. Lett.* **93**, 103903 (2004).
8. Kim, C., Kim, Y. J., Jang, E. S., Yi, G. C. & Kim, H. H. Whispering-gallery-mode-like-enhanced emission from ZnO nanodisk. *Appl. Phys. Lett.* **88**, 093104 (2006).

9. Yang, Y. H., Zhang, Y., Wang, N. W., Wang, C. X., Li, B. J. & Yang, G. W. ZnO nanocone: Application in fabrication of the smallest whispering gallery optical resonator. *Nanoscale* **3**, 592–597 (2011).
10. Yang, Y. H., Chen, X. Y., Feng, F. & Yang, G. W. Physical mechanisms of blue-shift of UV luminescence of a pencil-like ZnO nanowire. *Nano Lett.* **12**, 3879–3883 (2007).
11. Wang, N. W., Dong, J. W., Yang, Y. H., Li, B. J., Wang, C. X. & Yang, G. W. General strategy for nanoscopic light source fabrication. *Adv. Mater.* **23**, 2937–2941 (2011).
12. Ewald, P. P. Ueber die Grundlagen der Kristalloptik. *Ann. d. Physik* **354** (49), 1–38 (1916), (49), 117–143 (1916) and **355**, 519–556 (1917).
13. Oseen, C. W. Ueber die Wechselwirkung zwischen zwei elektrischen Dipolen der polarisationsebene in Kristallen und Flüssigkeiten. *Ann. d. Physik* **353** (17), 1–56 (1915).
14. Fung, A. K. & Chen, M. F. Numerical simulation of scattering from simple and composite random surfaces. *J. Opt. Soc. Am. A* **2**, 2274–2284 (1985).
15. Nieto-Vesperinas, M. & Soto-Crespo, J. M. Monte Carlo simulations for scattering of electromagnetic waves from perfectly conductive random rough surfaces. *Opt. Lett.* **12**, 979–981 (1987).
16. Liu, J. Z., Lee, S., Ahn, Y., Park, J. Y., Koh, K. H. & Park, K. H. Identification of dispersion-dependent hexagonal cavity modes. *Appl. Phys. Lett.* **92**, 263102 (2008).
17. Starykh, O. A., Jacquod, P. R. J., Narimanov, E. E. & Stone, A. D. Signature of dynamical localization in the resonance width distribution of wave-chaotic dielectric cavities. *Phys. Rev. E* **62**, 2078–2084 (2000).
18. Fang, W., Cao, H., Podolskiy, V. A. & Narimanov, E. E. Dynamical localization in microdisk lasers. *Opt. Express* **13**, 5641–5652 (2005).
19. Braun, I., Ihlein, G., Laeri, F., Nöckel, J. U., Schulz-Ekloff, G., Schüth, F., Vietze, U., Weiß, Ö. & Wöhrle, D. Hexagonal microlasers based on organic dyes in nanoporous crystals. *Appl. Phys. B* **70**, 335–343 (2000).

## Acknowledgements

This work was supported by NSFC (91232203, 11274396, 10804131, 11074311).

## Author contributions

G.W. Yang designed the experiments. N.W. Wang and Y.H. Yang performed the experiments. J.W. Dong and X.D. Chen carried out the theoretical study. G.W. Yang, J.W. Dong and C.X. Wang analysed the results. G.W. Yang and J.W. Dong wrote the paper. All the authors offer a critical review of the paper.

## Additional information

Supplementary information accompanies this paper at <http://www.nature.com/scientificreports>

**Competing financial interests:** The authors declare no competing financial interests.

**License:** This work is licensed under a Creative Commons Attribution-NonCommercial-NoDerivs 3.0 Unported License. To view a copy of this license, visit <http://creativecommons.org/licenses/by-nc-nd/3.0/>

**How to cite this article:** Wang, N.W. *et al.* Diffuse reflection inside a hexagonal nanocavity. *Sci. Rep.* **3**, 1298; DOI:10.1038/srep01298 (2013).